Self-assembled Ni/TiO_2 nanocomposite anodes synthesized *via* electroless plating and atomic layer deposition on biological scaffolds†

Konstantinos Gerasopoulos,[a] Xilin Chen,[b] James Culver,[c] Chunsheng Wang[b] and Reza Ghodssi*[a]

Received 1st June 2010, Accepted 13th August 2010
DOI: 10.1039/c0cc01689f

Ni(core)/TiO_2(shell) nanocomposite anodes were fabricated on three-dimensional, self-assembled nanotemplates of *Tobacco mosaic virus* using atomic layer deposition, exhibiting high capacities and rate capability and extremely low average capacity fading (~0.024% per cycle) for ~1000 cycles.

The development of next-generation Li-ion batteries is directly linked with the development of electrode materials and structures with enhanced energy and power density and long cycle life. Nanostructured materials have emerged as a promising solution due to the reduced distances for lithium ion diffusion, structural stability, as well as larger electrode/electrolyte contact area which increases the number of reaction sites.[1]

Recently, notable research interest has been directed towards the use of biological structures as templates for the synthesis of functional surfaces. This bio-inspired route offers added benefits such as simplicity, low cost, structural versatility as well as surface tunability of biological molecules to produce monodisperse nanoparticles.[2] Characteristic examples include the work by Nam *et al.* and Lee *et al.* who used engineered M13 bacteriophage viruses as templates to synthesize electrodes for Li-ion batteries and the investigation by Kim *et al.* who used peptides as sacrificial templates to form TiO_2 nanotubes.[3,4] These biotemplated materials are then mixed in powder form with polymer binders and carbon to fabricate electrodes using traditional ink-casting techniques, or alternatively attached through contact-printing on current collectors.[3c]

In this work, an alternative methodology that combines bottom-up biological self-assembly and metallization of *Tobacco mosaic virus* (TMV) scaffolds with nanofabrication for the direct synthesis of composite core/shell Ni-coated TMV/TiO_2 anodes on current collectors is presented. The TMV is a high aspect ratio cylindrical plant virus (300 nm in length, 18 nm diameter), which can be genetically modified to include cysteine residues that facilitate attachment of this rigid rod onto metal surfaces through thiol interactions and improve ion-binding affinity in electroless plating reactions. As a result, self-assembled metallic nanorods can be fabricated, which have been previously used by our group in proof-of-concept alkaline batteries.[5] Here, this bottom-up synthesis method is combined with Atomic Layer Deposition (ALD) for the development of functional Li-ion battery electrode surfaces with a metallic core/active material shell nanostructure. Such an architecture significantly enhances the electrochemical performance of electrodes as shown in the literature.[6] ALD was chosen due to its unique ability to produce uniform coatings on complex three-dimensional architectures.[7]

The material selected to demonstrate the concept of this synthetic pathway is titanium dioxide. TiO_2 has attracted attention as an anode alternative to carbon due to its safety and cyclic stability. Even though it has higher Li^+ insertion/deinsertion potential which reduces the energy density of the battery, lithium plating can be avoided; this results in cells with increased safety and stability.[8] While ALD has been previously employed by Kim *et al.*[4] and Cheah *et al.*[9] for the synthesis of TiO_2 anodes, the unique advantage of the proposed structure lies in the self-assembly of the viral materials. Nickel-coated TMV can be directly attached onto the metal substrate, thus forming a three-dimensional current collector for the deposition of the active material and enhancing the rate performance. Consequently, the requirement for binders and other conductive additives is negated, enhancing cycling stability. This property, combined with the selective patterning capabilities of the TMV using top-down lithography which have been demonstrated in prior work,[10] creates opportunities for integration of this method in large-scale manufacturing as well as microfabricated Li-ion batteries.

The nanostructured TiO_2 electrodes were fabricated on stainless steel discs (15.5 mm ø) where a gold layer is sputtered to facilitate TMV self-assembly. The nickel-coated TMV core was synthesized as previously described[5] followed by ALD coating of a 20 nm thick TiO_2 layer (details in the Supplementary Information). Finally, the electrodes were annealed in air at 450 °C for 3 h to facilitate formation of anatase phase which has been suggested as the most facile lithium ion intercalation host among the various polymorphs of TiO_2.[11] For comparison, electrodes without TMV were also fabricated by deposition of a TiO_2 film of similar thickness directly on the steel substrate. The mass of the active materials was measured by weighing the substrates before and after ALD with a high precision microbalance and was found to be 190–260 μg for the virus-structured anodes and ~30 μg for the thin films.

[a] *MEMS Sensors and Actuators Laboratory, Department of Materials Science and Engineering, Department of Electrical and Computer Engineering, Institute for Systems Research, University of Maryland, 2173 A.V. Williams Building, College Park, MD 20742, USA. E-mail: ghodssi@umd.edu; Tel: +1 301-405-8158*
[b] *Department of Chemical and Biomolecular Engineering, University of Maryland, College Park, MD 20742, USA*
[c] *Institute for Bioscience and Biotechnology Research, Department of Plant Science and Landscape Architecture, University of Maryland, College Park, MD 20742, USA*

† Electronic supplementary information (ESI) available: Experimental section, Fig. S1: EDS data, Fig. S2: XRD data, Fig. S3: Control charge/discharge, Fig. S4: Control CV scans, Fig. S5: Coulombic efficiency, Fig. S6: Post-testing SEM of electrode, Fig. S7: EIS data of samples. See DOI: 10.1039/c0cc01689f

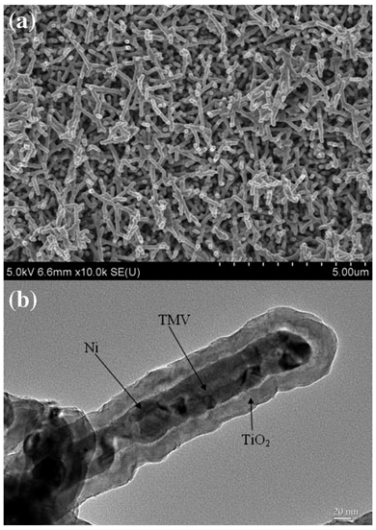

Fig. 1 (a) SEM image of the nanocomposite anode on the current collector; (b) cross-section TEM image of a single viral nanorod where the TMV (18 nm), Ni (~20 nm) and TiO_2 (~20 nm) are highlighted.

Fig. 1a shows an SEM image of the virus-templated nanomaterials after deposition of the TiO_2 layer on the nickel-coated TMV. The viruses attach onto the gold film from their 3′ (bottom) end based on a mechanism described in detail previously,[5] creating a three-dimensional, high surface area nanonetwork. The non-perfect vertical alignment is due to end-to-end attachment of more than one molecule as well as fragmentation inside the solution. Cross-section TEM of annealed nanowires was used to study the layer structure of the synthesized electrode. The image shown in Fig. 1b combined with Energy Dispersive X-ray Spectroscopy (EDS) data (Fig. S1) clearly illustrates the uniformity of Ni and TiO_2 coatings around the virus. It can also be observed that the thickness of the active electrode material is ~20 nm, indicating the high degree of control allowed during the ALD process. The effect of annealing the electrode was investigated using X-ray Diffraction (XRD) on as-prepared, annealed and control samples. Fig. S2 shows that the anatase peaks are detected only on the annealed sample.

The electrochemical properties of TiO_2 anodes with and without TMV were studied in half-cell coin batteries. Cyclic Voltammetry (CV) was used to examine the lithium intercalation/deintercalation reactions and the scans obtained at a rate of 0.5 mVs^{-1} from 2.6 V to 1 V (*vs.* Li^+/Li) are depicted in Fig. 2. A distinct pair of cathodic/anodic peaks centered around 1.68 V and 2.17 V respectively can be observed for both the planar TMV-modified TiO_2 electrodes, in good agreement with literature.[12] These peaks have an approximately two orders of magnitude larger height compared to the ones for the electrode without TMV, as shown in the inset of Fig. 2. This result may be attributed to the higher surface area of the nanostructured virus-templated anode.

The TiO_2 electrodes were galvanostatically cycled in the same voltage range to investigate the cycle life as well as the rate capability. The lithium insertion in the TiO_2 can be described by the following reaction:[11] $TiO_2 + xLi^+ + e^- \leftrightarrow Li_xTiO_2$ ($x \leq 0.5$). Lithium is inserted in the titanium dioxide lattice during discharge while extraction occurs during charge. Typical charge–discharge curves for the TMV-structured anode are

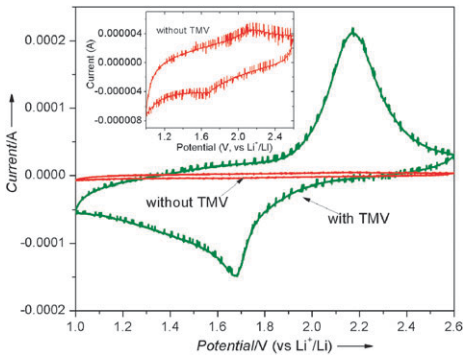

Fig. 2 CV scans for electrodes with (green) and without (red) TMV at a rate of 0.5 mVs^{-1}; the inset is an exploded view of the planar sample.

shown in Fig. 3 during the 1st, 2nd and 650th cycle at a current rate of 147 mAg^{-1}. As expected for anatase and in accordance with the CV data of Fig. 2, two plateaus appear during discharge and charge (around 1.75 V and 1.95 V respectively), suggesting a two-phase reaction. In this case, there is a transition from the tetragonal to orthorhombic phase as well as a separation into lithium rich and lithium poor domains.[14] The charge/discharge plateaus appear at lower/higher potentials compared to the CV scan due to the lower current density which results in lower overpotentials. Within the first 650 cycles of operation, the capacity drops from 223 $mAhg^{-1}$ in the 2nd cycle to 185 $mAhg^{-1}$ in the 650th cycle, indicating an average fading of only ~0.026% per cycle. In the bulk anatase structure the Li^+ insertion level x is 0.5 resulting in a theoretical capacity of ~168 $mAhg^{-1}$, however higher values can be obtained when the particle size is decreased to nanometre dimensions because extra Li^+ can be stored on the film surface and in the TiO_2 grain boundary.[11–13] It should be noted that the first insertion in the TiO_2 electrodes is accompanied by a side reaction converting some NiO to Ni that is present in the core as shown in Fig. S3, where a Ni-coated TMV control sample (without the TiO_2 layer) was cycled with the same current. This reaction is not fully reversible in the voltage range of 1–2.6 V [15] and results in an irreversible capacity that is observed in the first cycle for the virus-modified Ni/TiO_2 electrodes (Fig. 3). The irreversible nature of this reaction was further verified by CV scans that were performed on the control sample and are shown in Fig. S4. The coulombic efficiency for the $TMV/Ni/TiO_2$ rapidly rose to values exceeding 99.5% by the 13th cycle (Fig. S5).

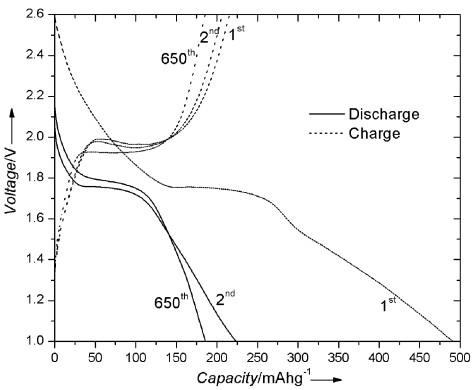

Fig. 3 Charge/discharge curves for the virus-structured anode at a rate of 147 mAg^{-1} for the 1st, 2nd and 650th cycle.

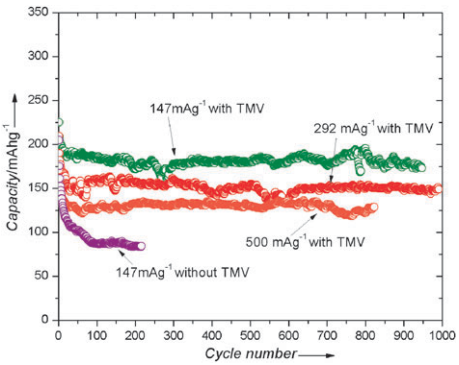

Fig. 4 Capacity *vs.* cycle number for electrodes with and without TMV.

Cycle life tests were performed at current rates of 147 mAg^{-1}, 292 mAg^{-1} and 500 mAg^{-1} and the discharge capacity is plotted in Fig. 4. The capacity for an anode without TMV at 147 mAg^{-1} is also presented for comparison. In the latter, the capacity stabilizes around 90 $mAhg^{-1}$ for this rate, while the nanostructured anodes show values of 180–185 $mAhg^{-1}$. The TMV-structured samples still notably outperform the planar films even at much higher currents. Due to this inferior performance, testing of the control sample was stopped after 230 cycles. In addition to the high capacity values, the stability of the electrodes is remarkable, since stable operation for several hundreds of cycles is demonstrated for all samples. Morphology examination of the anode that was cycled at 500 mAg^{-1} after 850 cycles using SEM shows retention of the three-dimensional structure of the TMV (Fig. S6). These observations highlight the importance of the proposed electrode: the robust metalized TMV template, which maintains its structural integrity after rigorous cycling, and the small volume expansion of TiO_2 that enables stable and reliable cycle-life operation create a unique anode with improved electrochemical performance.

In addition to the cycling stability test, the rate performance was also investigated (Fig. 5). In this experiment, the current was varied from 50 mAg^{-1} to 600 mAg^{-1} in increments of 5 cycles. The TMV-modified TiO_2 not only delivers at least two times higher capacity than regular TiO_2 film, but also provides enhanced rate capacity. At high current densities of 300 and 600 mAg^{-1}, the capacity for the virus-templated electrodes is more than three times greater compared to the thin film anode. The high rate performance of TMV/Ni/TiO_2 is attributed to the low impedance, as demonstrated by Electrochemical Impedance Spectroscopy (EIS) experiments (Fig. S7).

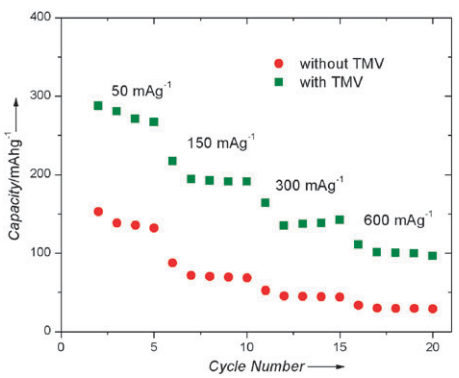

Fig. 5 Rate capability for electrodes with and without TMV.

In summary, a Ni/TiO_2 nanocomposite anode using the *Tobacco mosaic virus* was presented. The rigid rod structure of the TMV allows formation of self-assembled, three-dimensional nickel nanonetworks which are attached directly onto current collectors and coated uniformly with an ALD TiO_2 layer without the need for binders and other additives. Comparison with thin film electrodes showed improved capabilities and reaction kinetics. The synthesis of the viral nanorods is simple, versatile and can be incorporated into batch nanofabrication processes.

This work was supported by the Laboratory for Physical Sciences, NSF Nanomanufacturing Program (NSF-CMMI 0927693), Maryland Tedco and Department of Energy (FG0202ER45975). The authors acknowledge the staff at Maryland Nanocenter and Dr Li-Chung Lai at the NISP Lab for assisting with TEM imaging. Also, Dr Peter Zavalij for help with the XRD data and Professor Peter Kofinas for providing access to a high precision microbalance.

Notes and references

1 C. Jiang, E. Hosono and H. Shu, *Nano Today*, 2006, **1**, 28–33; P. G. Bruce, B. Scrosati and J.-M. Tarascon, *Angew. Chem., Int. Ed.*, 2008, **47**, 2930–2946; Y.-G. Guo, J.-S. Hu and L.-S. Wan, *Adv. Mater.*, 2008, **20**, 2878–2887.
2 N. Ma, E. H. Sargent and S. O. Kelley, *J. Mater. Chem.*, 2008, **18**, 954–964; S. Sotiropoulou, Y. Sierra-Sastre, S. S. Mark and C. A. Batt, *Chem. Mater.*, 2008, **20**, 821–834.
3 K. T. Nam, D. W. Kim, P. J. Yoo, C. Y. Chiang, N. Meethong, P. T Hammond, Y. M. Chang and A. M. Belcher, *Science*, 2006, **312**, 885–888; Y. J. Lee, H. Yi, W. Kim, K. Kang, D. S. Yun, M. S. Strano, G. Ceder and A. M. Belcher, *Science*, 2009, **324**, 1051–1055; K. T. Nam, R. Wartena, P. J. Yoo, F. Liau, Y. J. Lee, Y. M. Chiang, P. Hammond and A. M. Belcher, *Proc. Natl. Acad. Sci. U. S. A.*, 2008, 107.
4 S.-W. Kim, T. H. Han, J. Kim, H. Gwon, H.-S. Moon, S.-W. Kang, S. O. Kim and K. Kang, *ACS Nano*, 2009, **3**, 1085–1090.
5 E. Royston, A. Ghosh, P. Kofinas, M. T. Harris and J. N. Culver, *Langmuir*, 2008, **24**, 906–912; K. Gerasopoulos, M. McCarthy, E. Royston, J. N. Culver and R. Ghodssi, *J. Micromech. Microeng.*, 2008, **18**, 104003.
6 J. Liu, W. Li and A. Manthiram, *Chem. Commun.*, 2010, **46**, 1437–1439.
7 P. Banerjee, I. Perez, L. Henn-Lecordier, S. B. Lee and G. W. Rubloff, *Nat. Nanotechnol.*, 2009, **4**, 292–296.
8 Y.-G. Guo, Y.-S. Hu, W. Sigle and J. Maier, *Adv. Mater.*, 2007, **19**, 2087–2091; G. F. Ortiz, I. Hanzu, T. Djenizian, P. Lavela, J. L. Tirado and P. Knauth, *Chem. Mater.*, 2009, **21**, 63–67.
9 S. K. Cheah, E. Perre, M. Rooth, M. Fondell, A. Harsta, L. Nyholm, M. Boman, T. Gustafsson, J. Lu, P. Simon and K. Edstrom, *Nano Lett.*, 2009, **9**, 3230–3233.
10 K. Gerasopoulos, M. McCarthy, P. Banerjee, X. Fan, J. N. Culver and R. Ghodssi, *Nanotechnology*, 2010, 21.
11 Z. Yang, D. Choi, S. Kerisit, K. M. Rosso, D. Wang, J. Zhang, G. Graff and J. Liu, *J. Power Sources*, 2009, **192**, 588–598; J. Xu, Y. Wang, Z. Li and W. F. Zhang, *J. Power Sources*, 2008, **175**, 903–908.
12 L. Kavan, J. Rathousky, M. Graetzel, V. Shklover and A. Zukal, *J. Phys. Chem. B*, 2000, **104**, 12012–12020.
13 M. Wagemaker, W. J. H. Borghols and F. M. Mulder, *J. Am. Chem. Soc.*, 2007, **129**, 4323–4327.
14 D. Wang, D. Choi, J. Li, Z. Yang, Z. Nie, R. Kou, D. Hu, C. Wang, L. V. Saraf, J. Zhang, I. A. Aksay and J. Liu, *ACS Nano*, 2009, **3**, 907–914.
15 E. Hosono, S. Fujihara, I. Honma and H. Zhou, *Electrochem. Commun.*, 2006, **8**, 284–289.